Spatial assessment of long-term vent opening probability in the Long Valley volcanic region (CA, USA)

A research study in collaboration with:
Marcus Bursik[(1)], Abani K. Patra[(2)], E. Bruce Pitman[(3)]

(1) University at Buffalo, Department of Geology
(2) University at Buffalo, Department of Mechanical and Aerospace Engineering
(3) University at Buffalo, Department of Materials Design and Innovation

Project Hazard SEES: Persistent volcanic crises resilience in the face of prolonged and uncertain risk,
National Science Foundation, 2015 - 2018.

EAST TENNESSEE STATE UNIVERSITY

Volcanology Seminar
19 April 2017, Department of Geosciences, ETSU

- The Long Valley volcanic region -

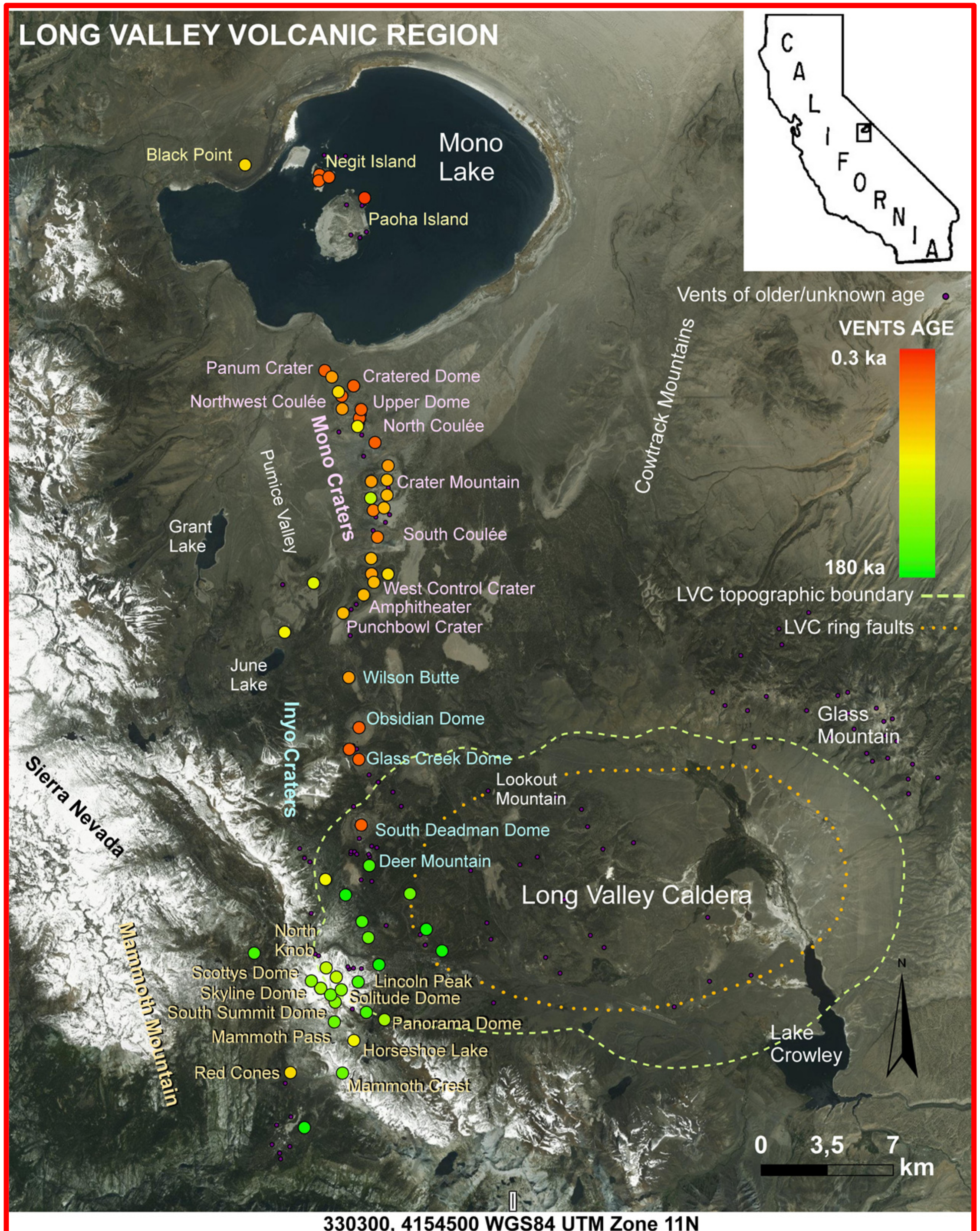

Long Valley caldera (LVC), was created by the eruption of >200km^3 tephra ~ 760ka BP (Bishop tuff).

Over the last 180ka the eruptions have been mostly localized at **Mammoth Mountain,** on the western rim of LVC and along the **Mono-Inyo Craters** volcanic chain, stretching ~45km North towards Mono lake.

The most recent period of **unrest started in 1978** - several seismic swarms in LVC and below Mammoth mountain, and diffuse volcanic CO_2 emissions.

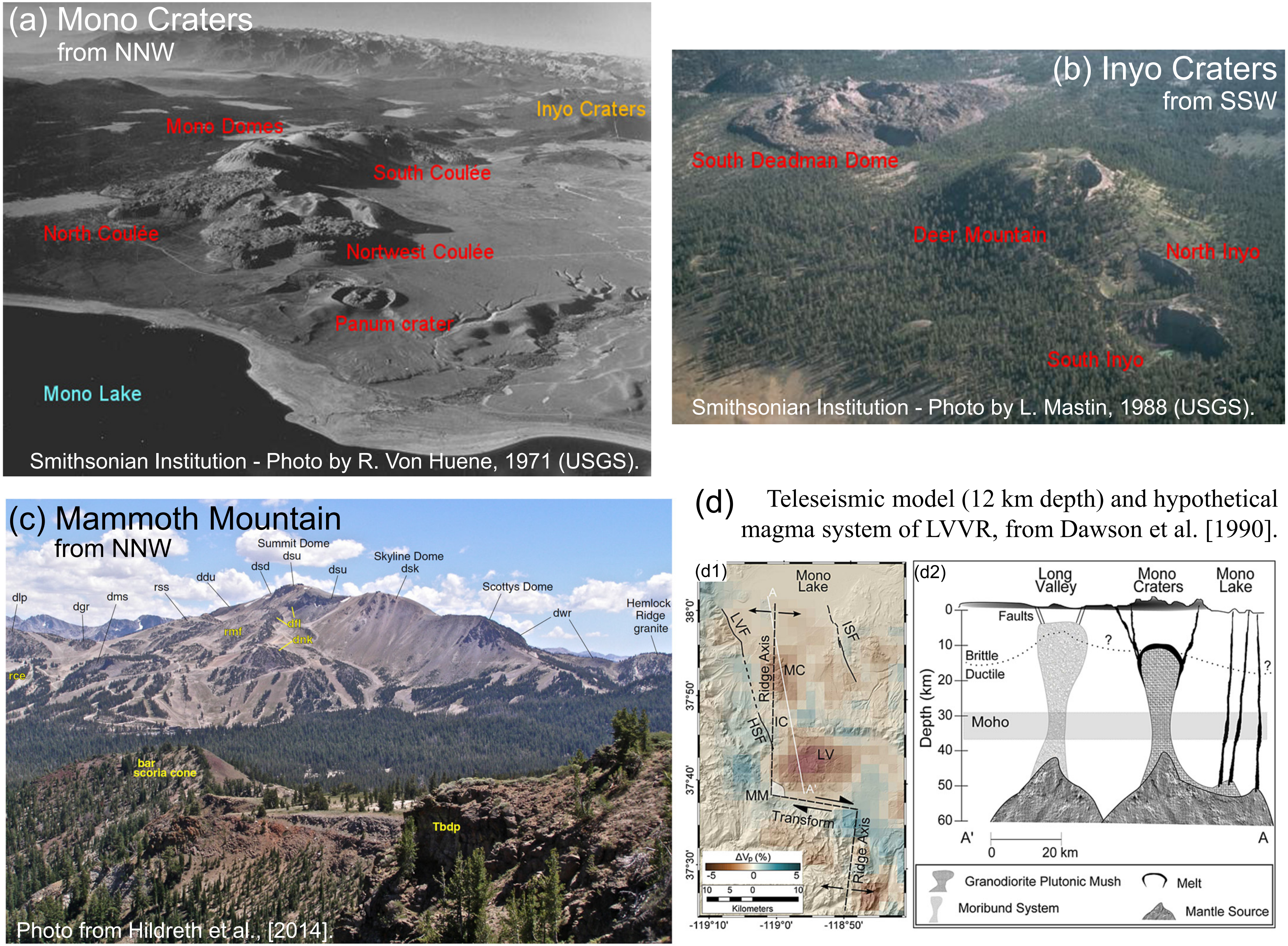

(a) Mono Craters
from NNW
Inyo Craters
Mono Domes
South Coulée
North Coulée
Nortwest Coulée
Panum crater
Mono Lake
Smithsonian Institution - Photo by R. Von Huene, 1971 (USGS).
(b) Inyo Craters
from SSW
South Deadman Dome
Deer Mountain
North Inyo
South Inyo
Smithsonian Institution - Photo by L. Mastin, 1988 (USGS).
(c) Mammoth Mountain
from NNW
Summit Dome
dsu
dsd
dsu
Skyline Dome
dsk
Scottys Dome
dlp
dgr
dms
rss
ddu
rmf
dfl
dnk
dwr
Hemlock Ridge granite
rce
bar
scoria cone
Tbdp
Photo from Hildreth et al., [2014].
(d) Teleseismic model (12 km depth) and hypothetical magma system of LVVR, from Dawson et al. [1990].
(d1)
Mono Lake
A
LVF
ISF
Ridge Axis
MC
HSF
IC
LV
A'
MM
Transform
Ridge Axis
ΔVp (%)
-5 0 5
10 5 0 10
Kilometers
38°0'
37°50'
37°40'
37°30'
-119°10'
-119°0'
-118°50'
(d2)
Long Valley
Mono Craters
Mono Lake
Faults
Brittle
Ductile
Moho
Depth (km)
0
10
20
30
40
50
60
A'
A
0
20 km
Granodiorite Plutonic Mush
Moribund System
Melt
Mantle Source

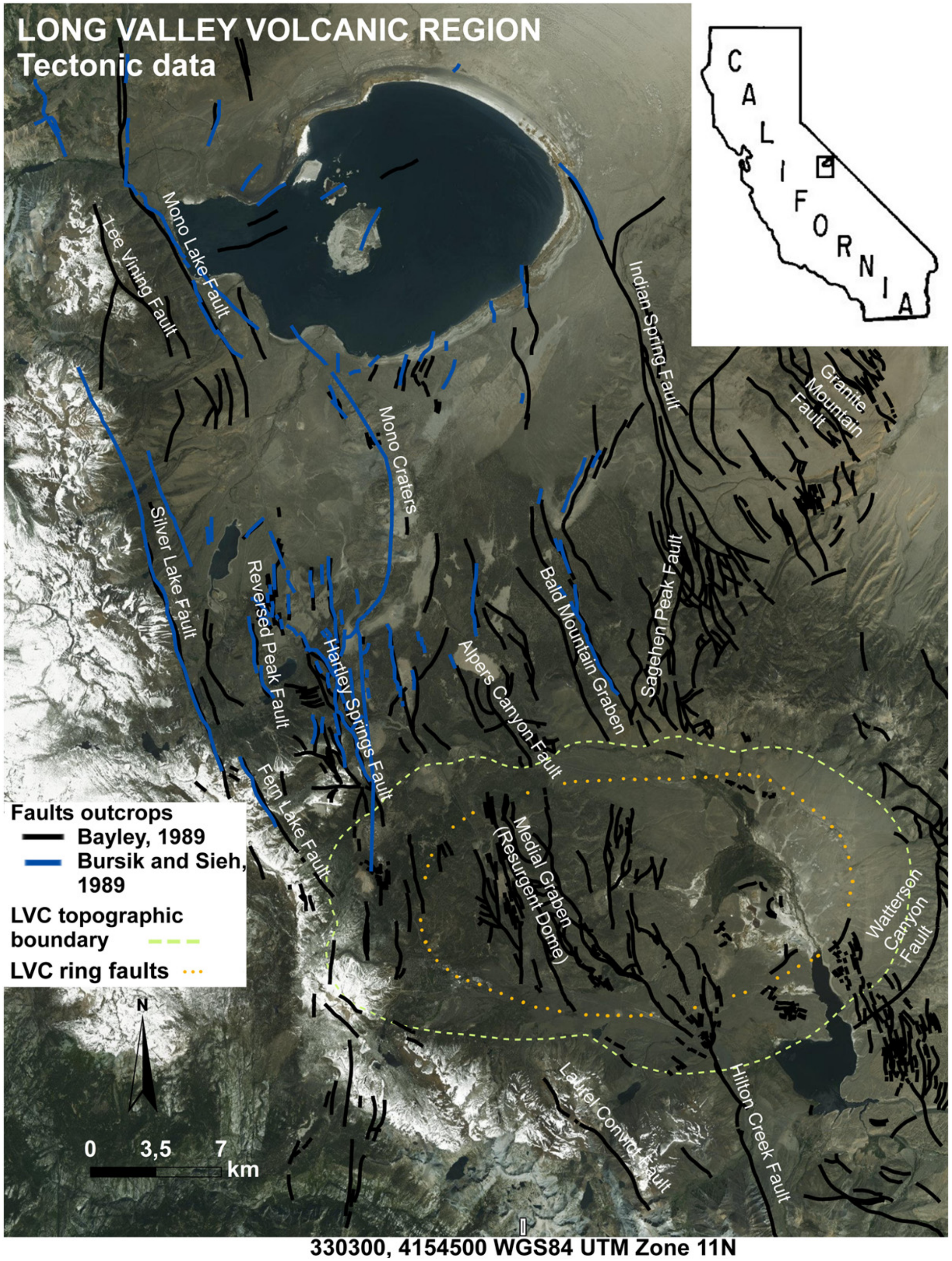

(b) Conceptual geologic model based on the electric resistivity features of Mono region. From Peacock et al., [2015].

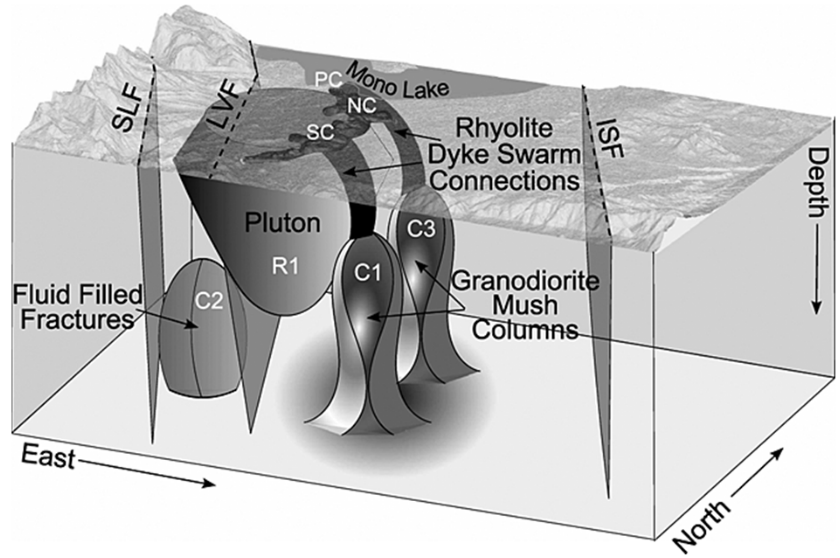

(c) Schematic of the electric resistivity model and hydrothermal flow of LVC region. Arrow colors represent temperature, in purple is the paleohydrothermal flow. From Peacock et al., [2016]

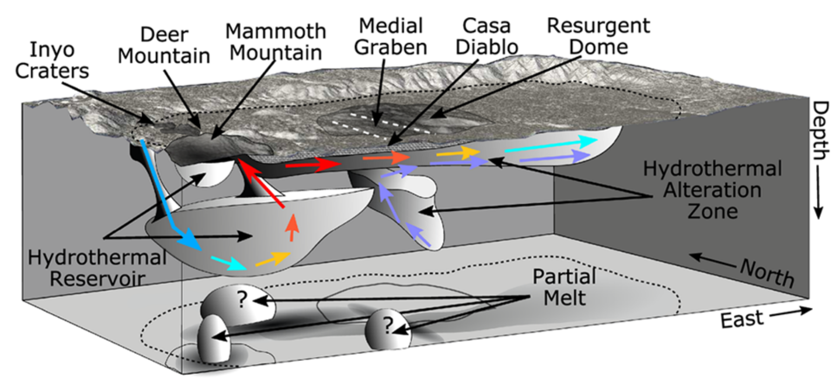

- Eruptive record description -

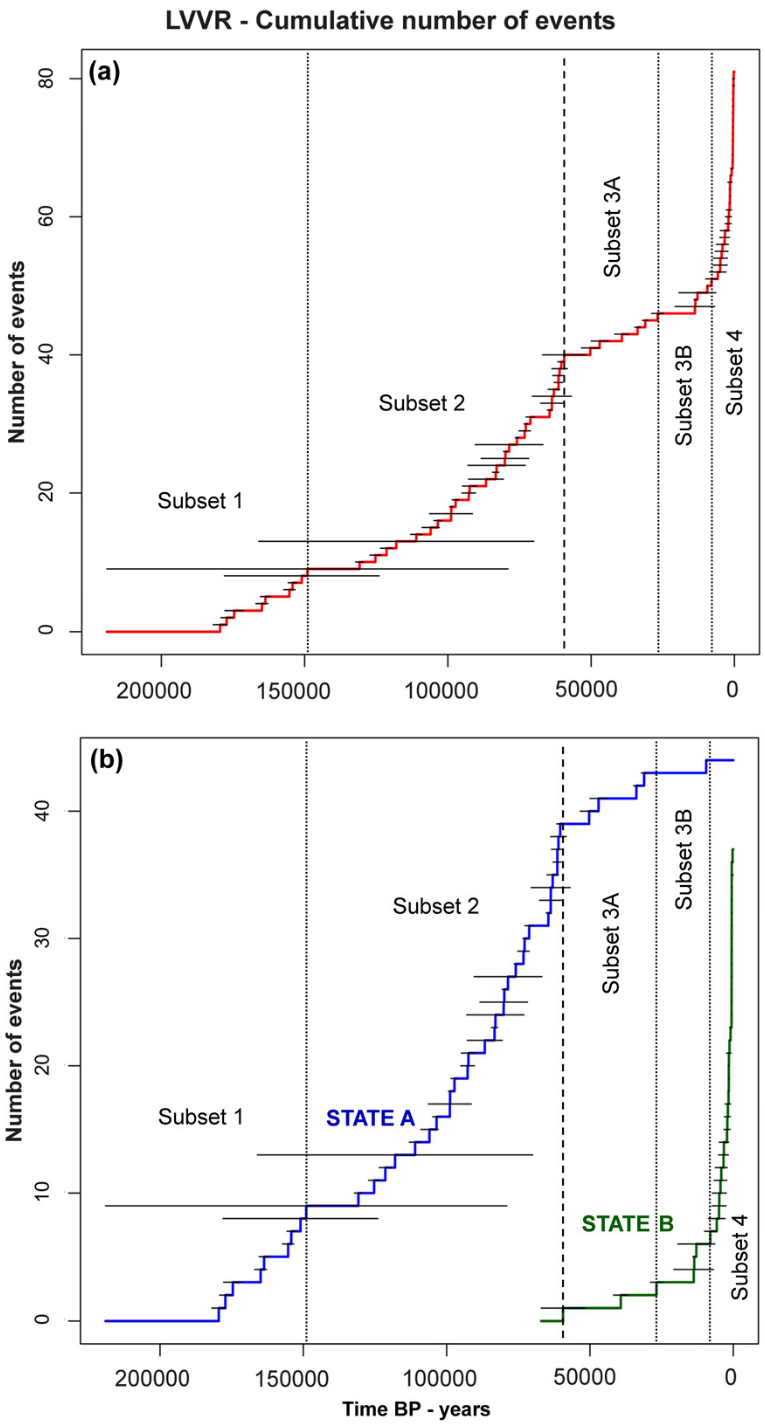

TEMPORAL RECORD

Past record was divided into five subsets.

A

1) 180/149 ka - 9 events. average return time ~3,400 yrs, concluded with a ~18 kyr period of quiescence.

2) 131/60 ka - 30 events, average return time ~2,350 yrs, concluded by a ~ 20 km location shift to the first Mono event.

3A) 59/27 ka - 7 events, average return time ~4,650 yrs, concluded by a ~13 kyr period of quiescence.

B

3B) 14/8 ka - 5 events, average return time ~1,150 yrs, concluded by a relative increase of activity rate.

4) < 6 ka - 30 events, average return time ~200 yrs, more than 10 vents active together at 625-600 yr BP.

We consider **two states** of volcanic activity, A and B, with an unknown chance of a new event occurring in State A.

The State A concerns the **Mammoth Mountain** area, whereas the State B the more recently active **Mono basin**, with Inyo Craters lying in the middle.

The separation at ~60ka corresponds with the **activation of the northern part** of the region.

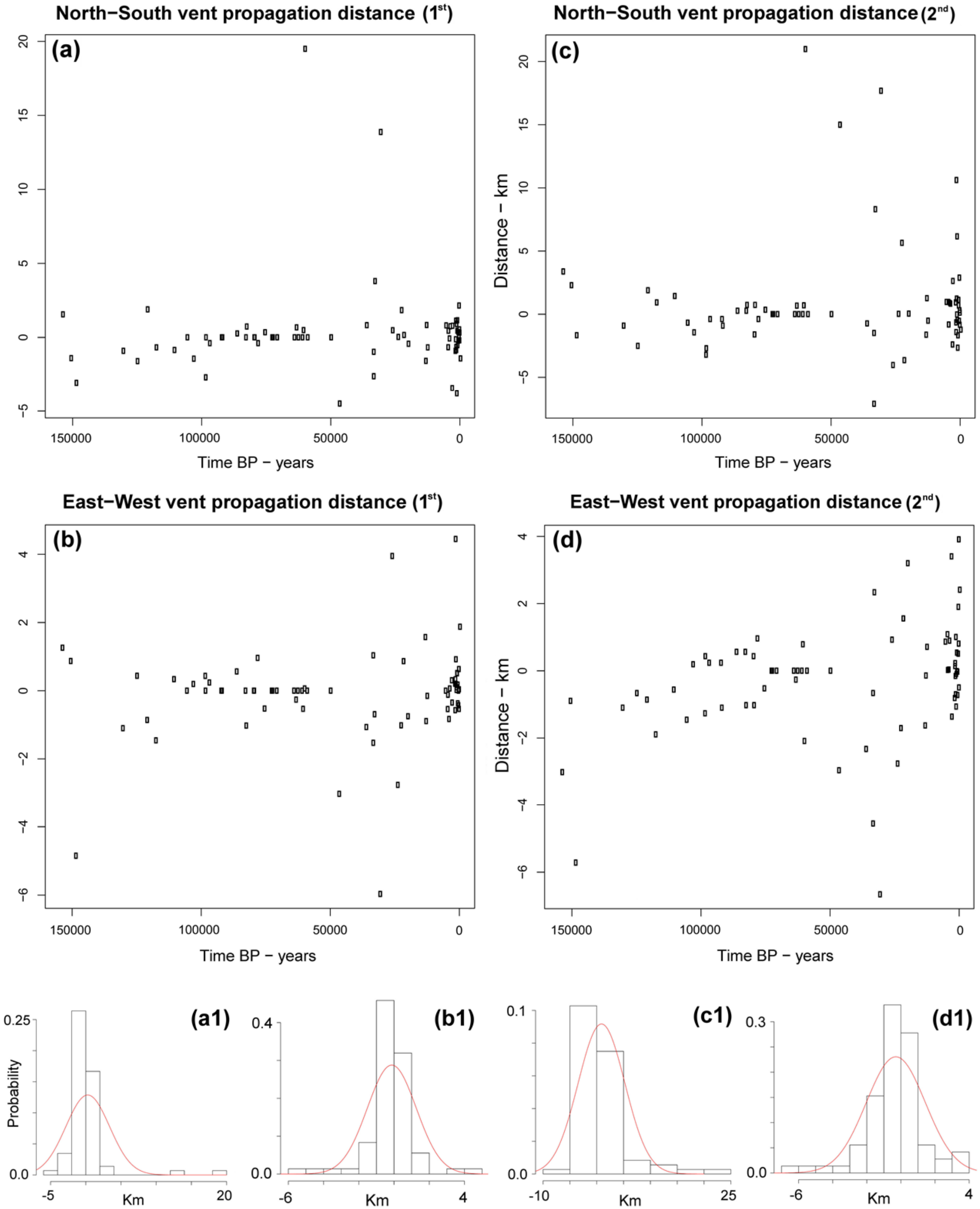

DISTANCES OF PROPAGATION

Alternative distances are easily defined: the spatially closest preexisting vent, the second closest vent, etc.

A **20km jump** in the N/S distance of propagation is noticed around 60ka.

The vent propagation process is likely Gaussian, and the N/S scale is ~5 times larger than the E/W scale.

There is a significant increase of N/S propagation distances after such jump.

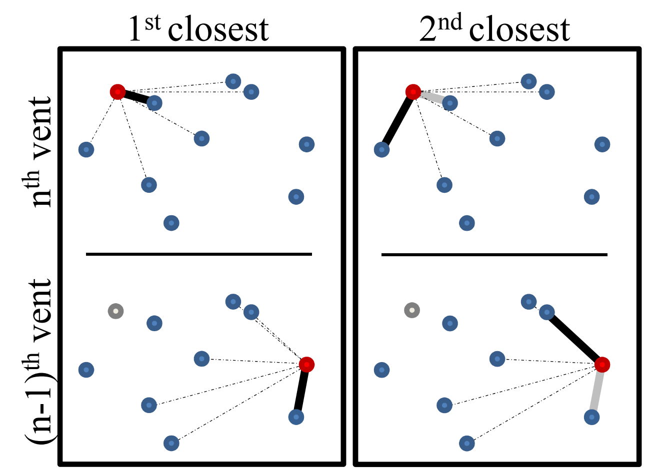

Examples of 1st and 2nd spatially closest preexisting vents.

- Spatial modeling: vent opening probability maps -

Doubly stochastic vent opening maps

A "map of vent opening" is the **spatial estimate** of the probability of vent opening per km^2 in each point of the region of interest.

That probability is **conditional** on the occurrence of a new eruption, without a temporal window.

The volcano is presented as a **random system** that must be assessed with **uncertain information**.

Adopting a **doubly stochastic approach,** some ill-constrained parts of the long-term probability models will be randomly changed, reporting the effect on the probability estimates.

As a consequence of this approach, some probability estimates will have their own confidence intervals.

Even the final probability maps will be affected by uncertainty: we calculate the **mean, 5^{th} and 95^{th} percentile** values for the vent opening probability density functions.

Three different models and the four uncertainty sources

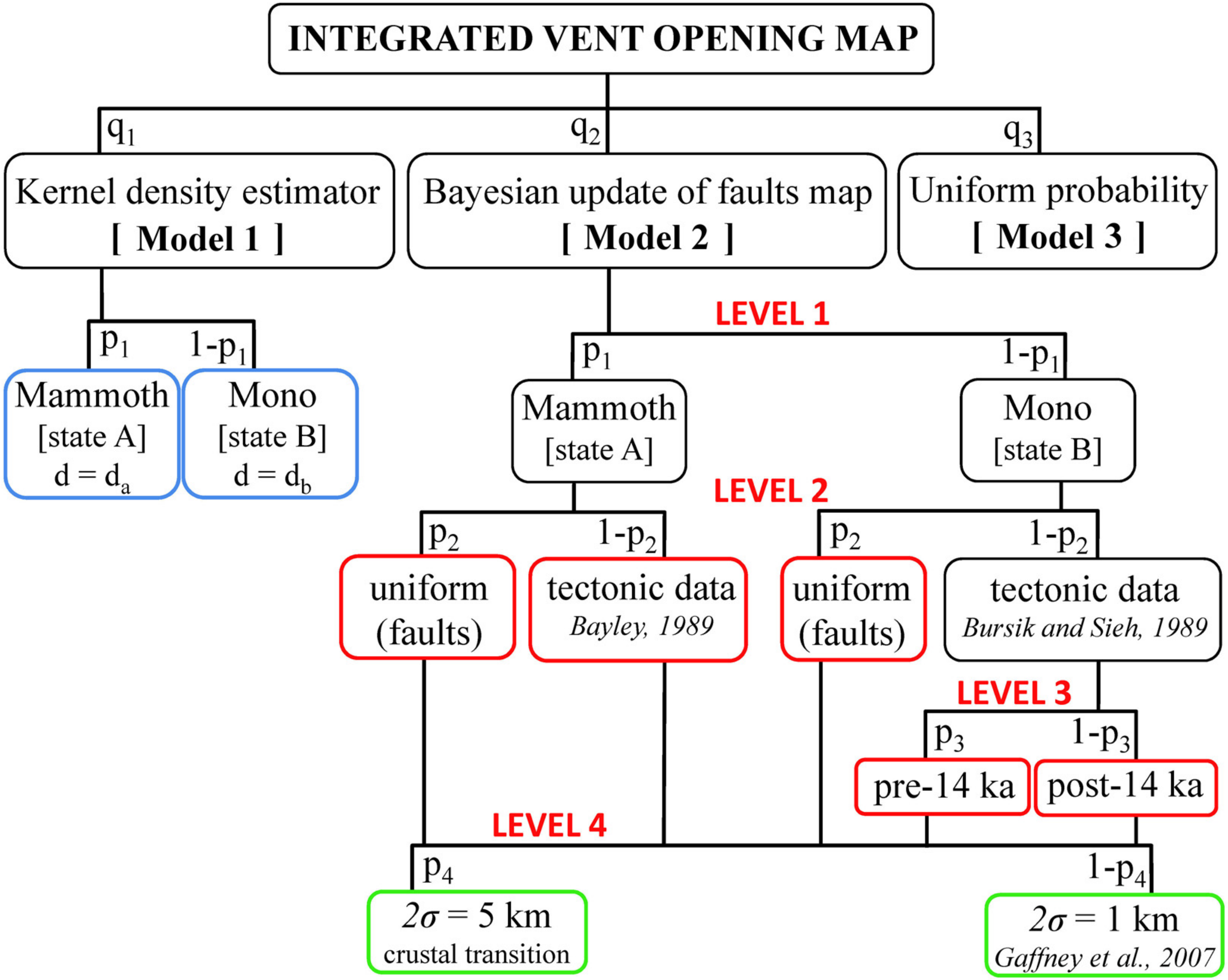

- Model 1: Gaussian kernel density estimator -

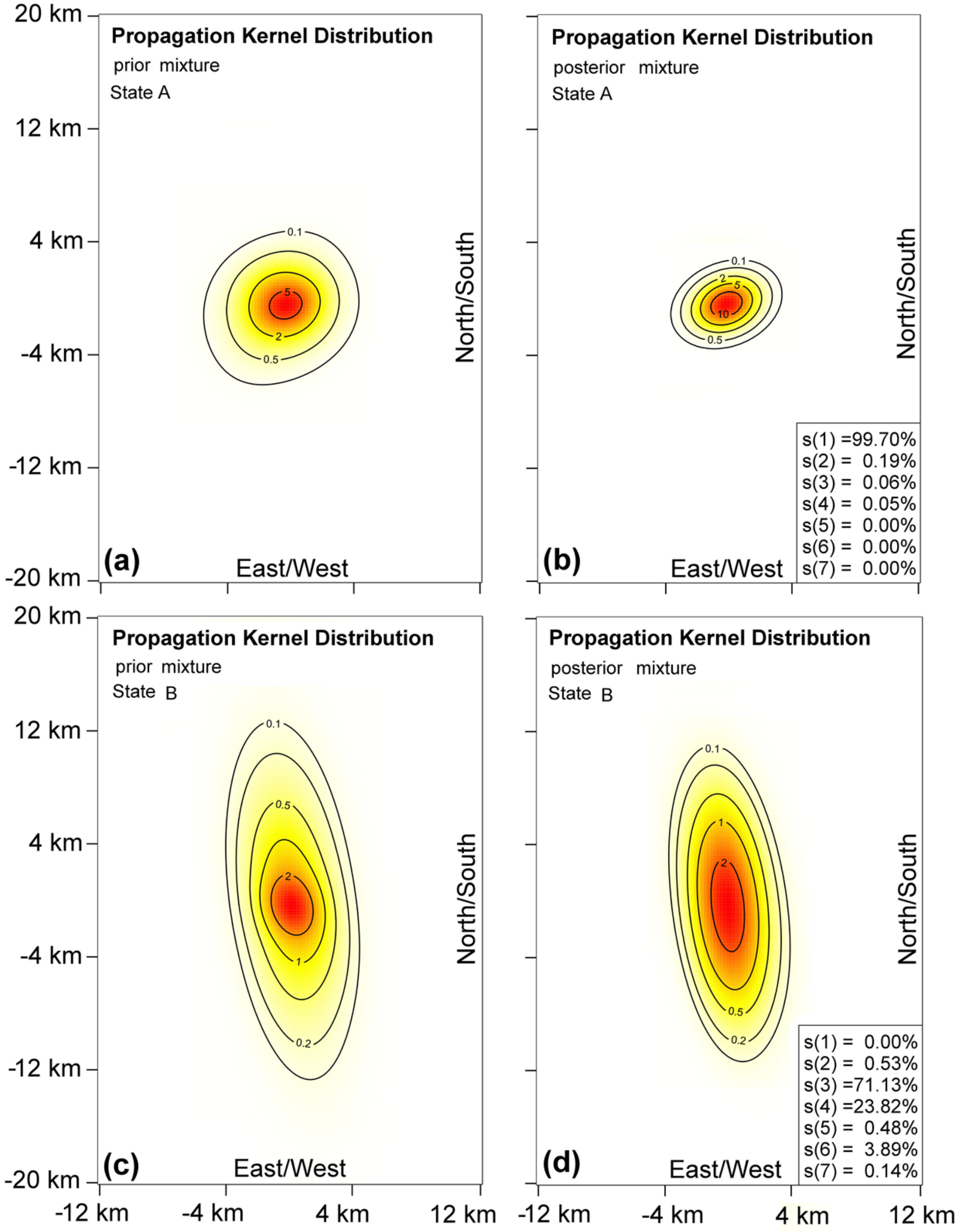

KERNEL FUNCTIONS

Given the locations $(x_i, y_i)_{i=1,\ldots,N}$ of the past N events, a new event propagates from one event location **randomly chosen** from the preexisting, to a **random distance**:

$$\boldsymbol{X} = (x_{\boldsymbol{k}} + d_1,\ y_{\boldsymbol{k}} + d_2),$$

where $\boldsymbol{X}$ is the spatial location of the next vent,

$\boldsymbol{k}$ is a discrete random variable in $\{1,\ldots,N\}$ sampling one of the previous vents,

$\boldsymbol{d} = (d_1, d_2)$ is a two dimensional Gaussian random vector with mean μ and covariance matrix Σ.

The random variable $\boldsymbol{d}$ changes according with the state - in the figure are presented the statistics of the past propagation distances.

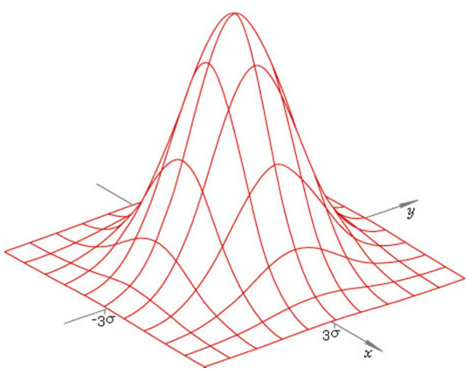

Example of Gaussian density plot.

Vent opening probability maps - Model 1 (kernel density estimator)

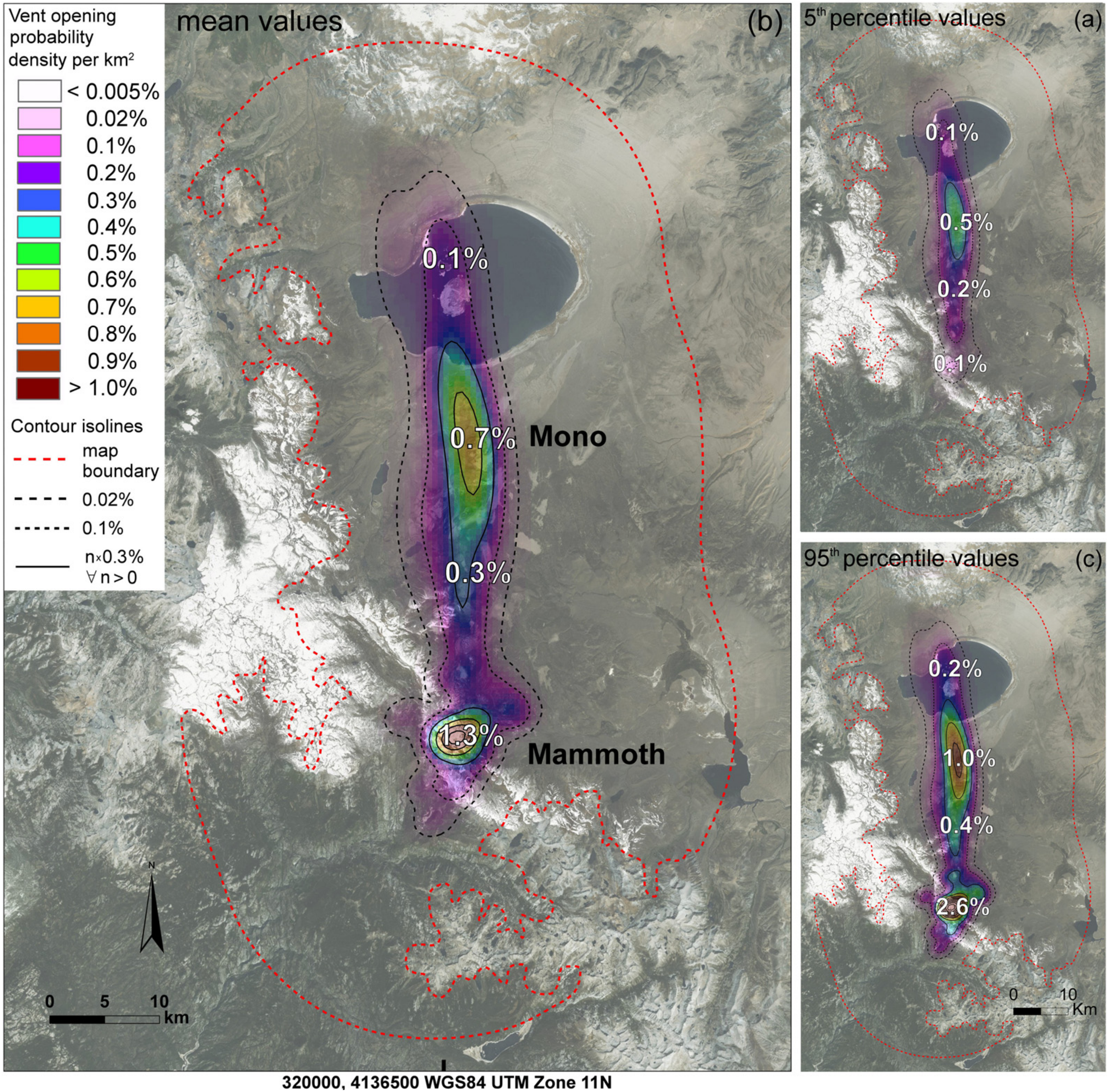

We obtain the density f of $\boldsymbol{X}$ by convolving the **probability kernel** describing $\boldsymbol{d}$ with the past vent location sites.

The importance of vent locations belonging to the **Mammoth Mountain** region ranges from a negligible value to equal importance with the ones in the more recently active **Mono region**.

A **Monte Carlo sampling** explores this uncertainty source.

- Model 2: Bayesian update of fault map -

The vent opening map is assumed to depend on a **tectonic parameter** $\zeta = (\zeta_1, \zeta_2)$, which is the outcrop of the fault interacting with a future potential rising dike.

The model assumes that the new vents will likely **open near** the unknown location of ζ.

The prior distribution of ζ is the linear combination of **log-extension data** and uniform distributions representing **missing information**.

Conditioned on ζ, the likelihood for vent location is a symmetric **Gaussian function** of mean ζ and covariance matrix $\sigma^2\mathbf{I}$.

Two alternative models are used to constrain the standard deviation σ.

σ relates to the expected distance from the fault outcrops to the vent openings:

- 10 km depending on the **brittle/ductile transition** depth, or

- 2 km depending on **numerical models** for dike propagation.

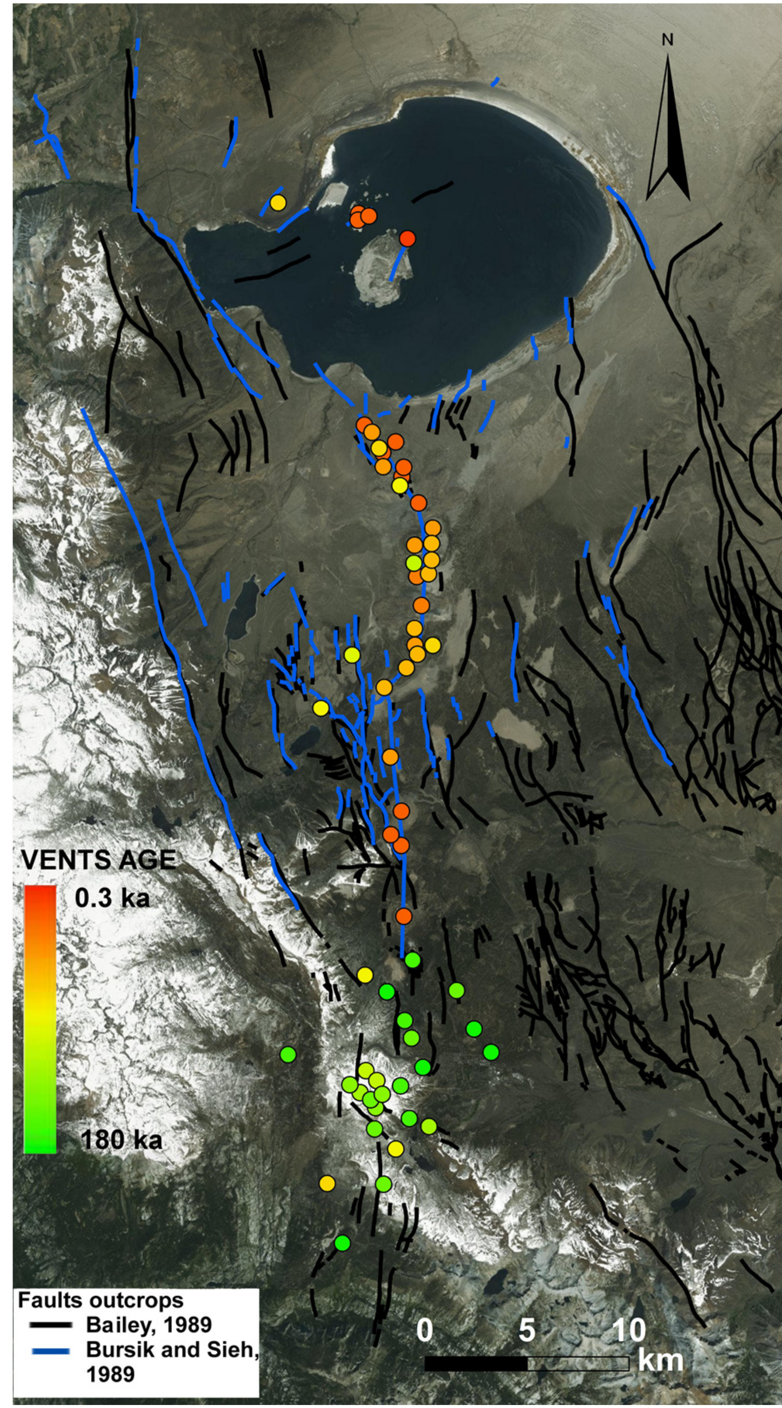

Tectonic parameter ζ (posterior probability map)

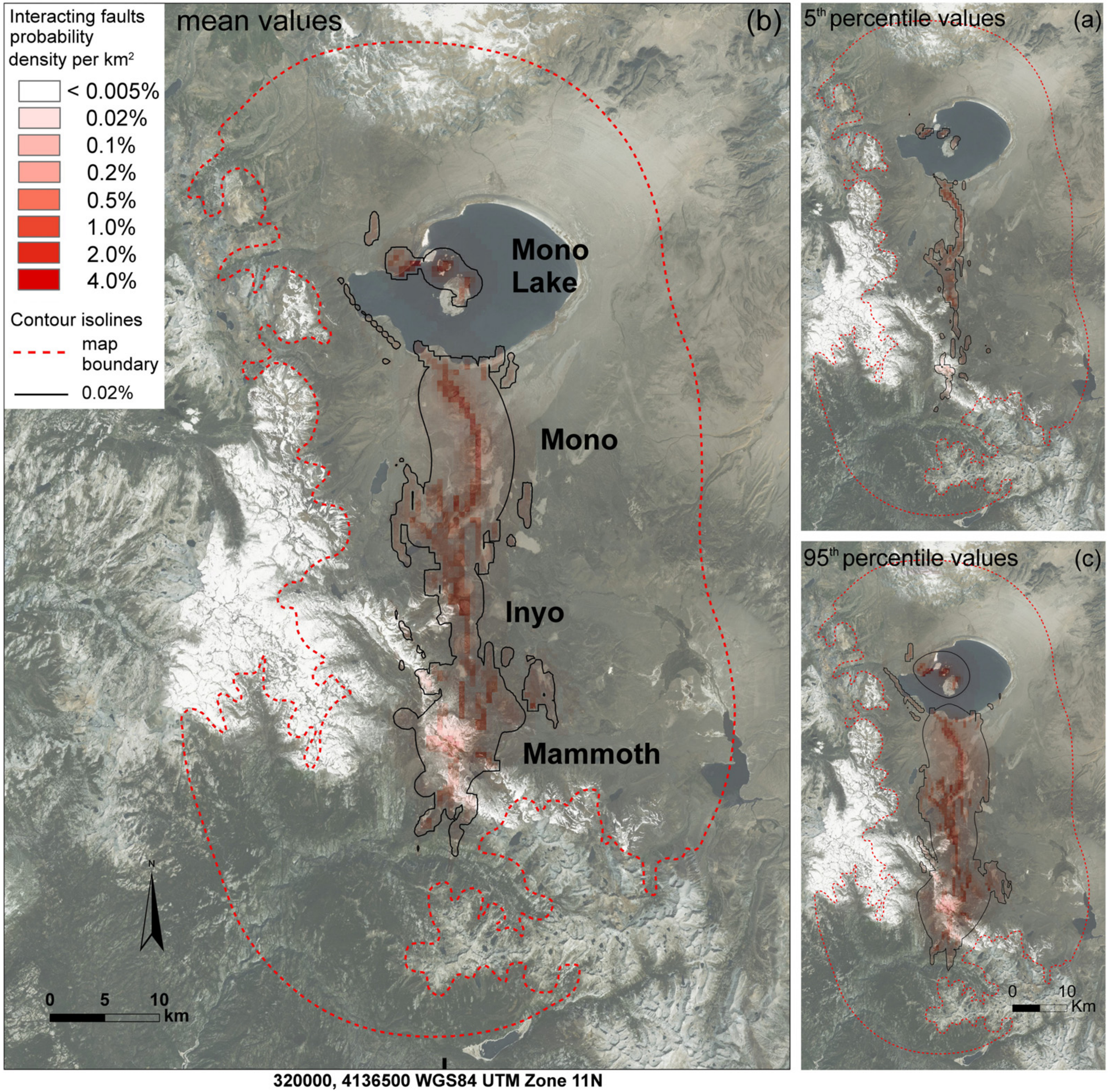

The Bayes Theorem enables us to calculate the **posterior** probability density of *ζ* as the **product** of its prior probability and the likelihood functions near past vents locations.

It describes the fault locations that lie **closer to past events.**

The presented map includes either the **uncertainty sources** concerning tectonic data (σ model, age window, incompleteness), and Mammoth Mountain unknown relevance.

Vent opening probability maps - Model 2 (Bayesian update of faults map)

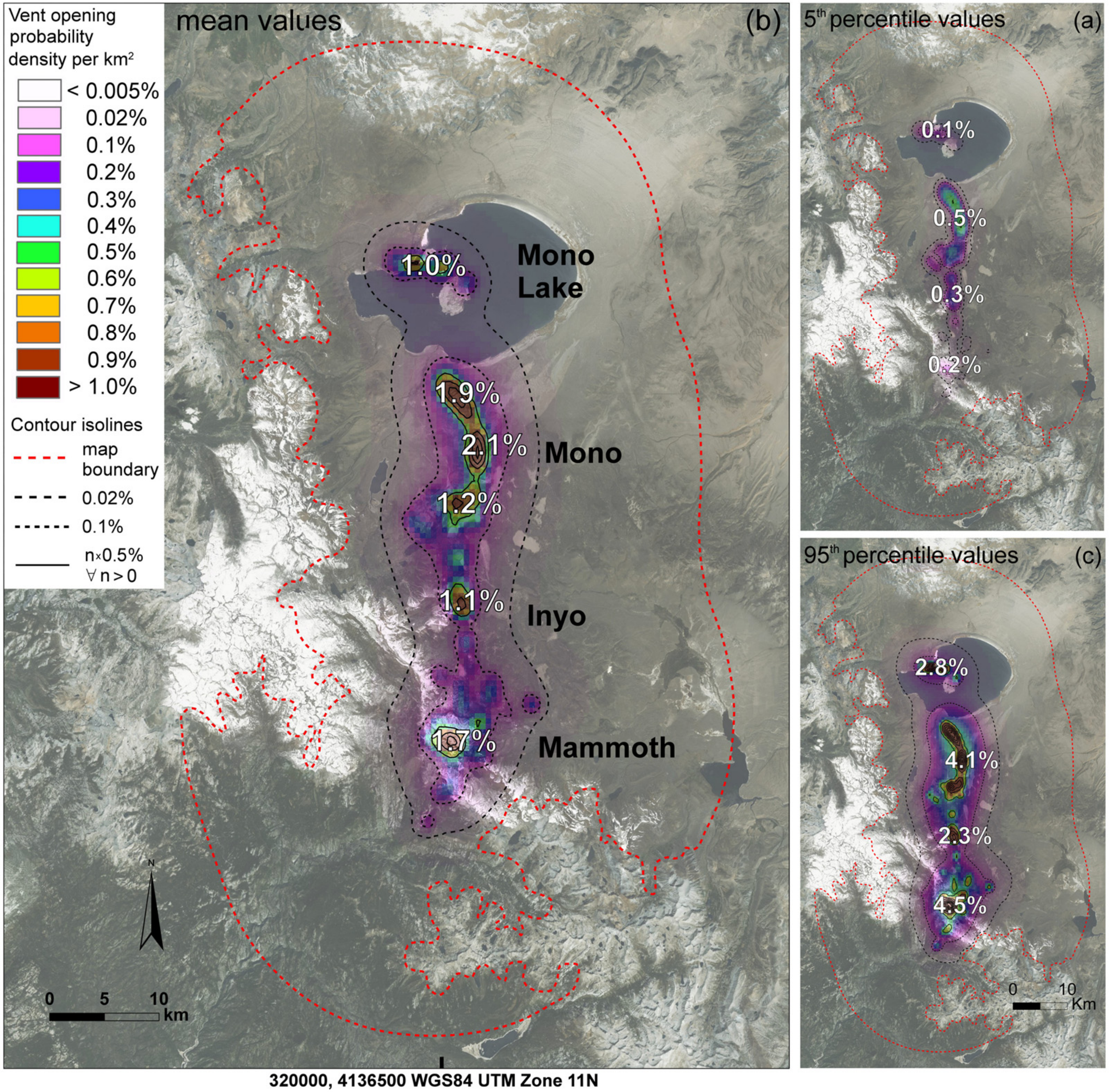

The density f of $\boldsymbol{X}$ according to Model 2 is obtained by convolving the **likelihood kernel** with the posterior ζ map.

Everything is done inside a **Monte Carlo sampling** that varies the uncertainty parameters.

- Models integration: Bayesian Model Averaging -

Bayesian model averaging (BMA)

Let $(M_i)_{i=1,\dots,n}$ be different probability models - BMA enables us to define some **performance scores** $[s(i)]_{i=1,\dots,n}$ for them based on the available observations *D,* e.g. the past vent locations.

Equal prior scores $[s(i)]_{i=1,\dots,n}$ are assumed for the models, such that $s_i = 1/n$ for all *i*.
The Bayes Theorem states that, for each $i=1,\dots,n$, the posterior scores are:

$$s(i|D) = \frac{L_i(D) \cdot s(i)}{C},$$

where L_i is the likelihood associated to model *i*, and *C* is a normalizing constant such that the new weights still sum to one.

The posterior scores are proportional to the **likelihood** that the models give to the observed data.

The averaged model is defined by the **linear combination** of the outputs given by the different models, with the scores $[s(i|D)]_{i=1,\dots,n}$ as weighting coefficients.

Vent opening probability maps - Averaged model

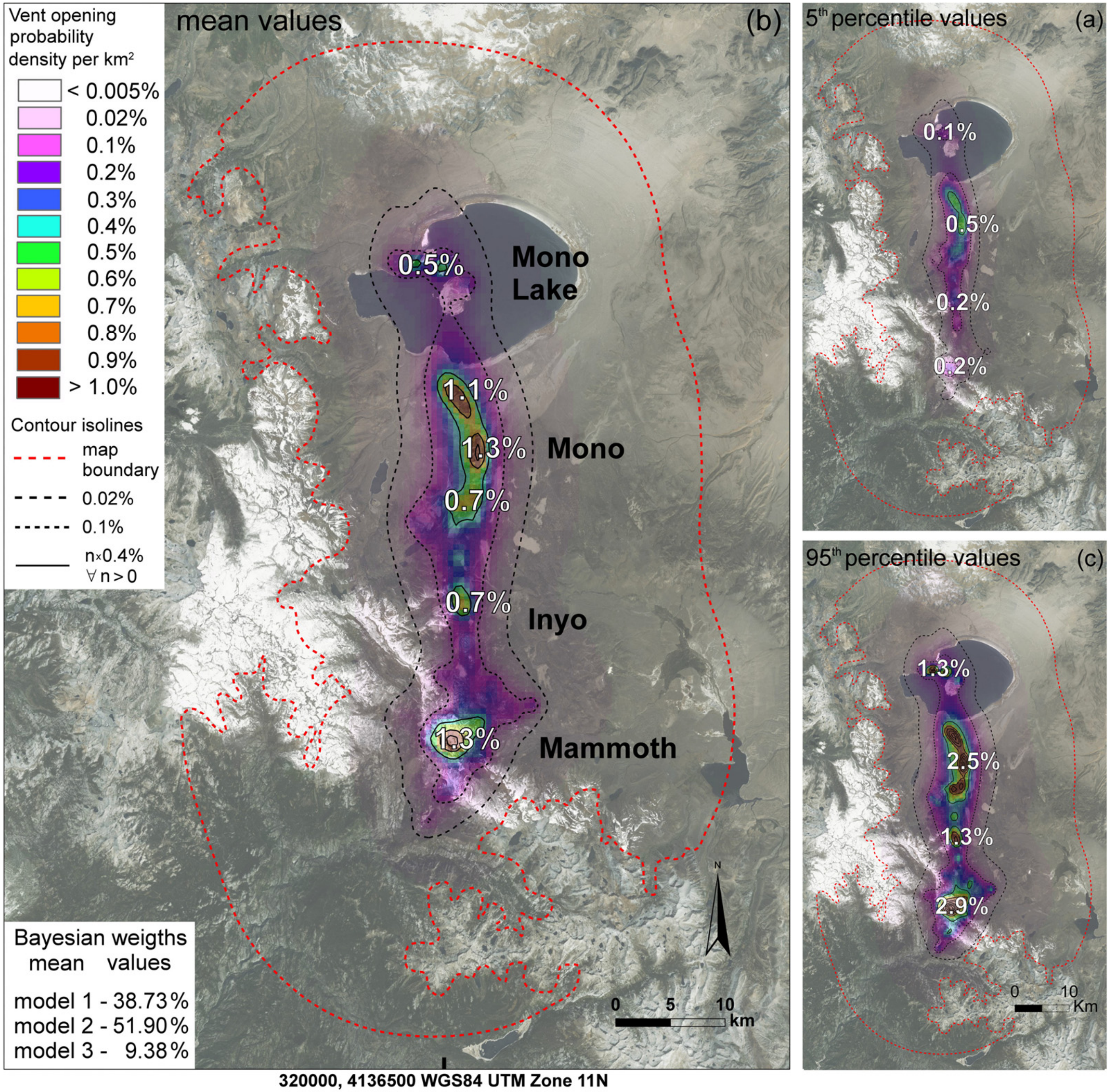

Through the BMA we obtain the modeling **performance scores** of
the three different models.

MODEL 1 - q_1
kernel density estimator

MODEL 2 - q_2
Bayesian update of faults map

MODEL 3 - q_3
Uniform probability map

	mean
q_1	38.73%
q_2	51.90%
q_3	9.38%

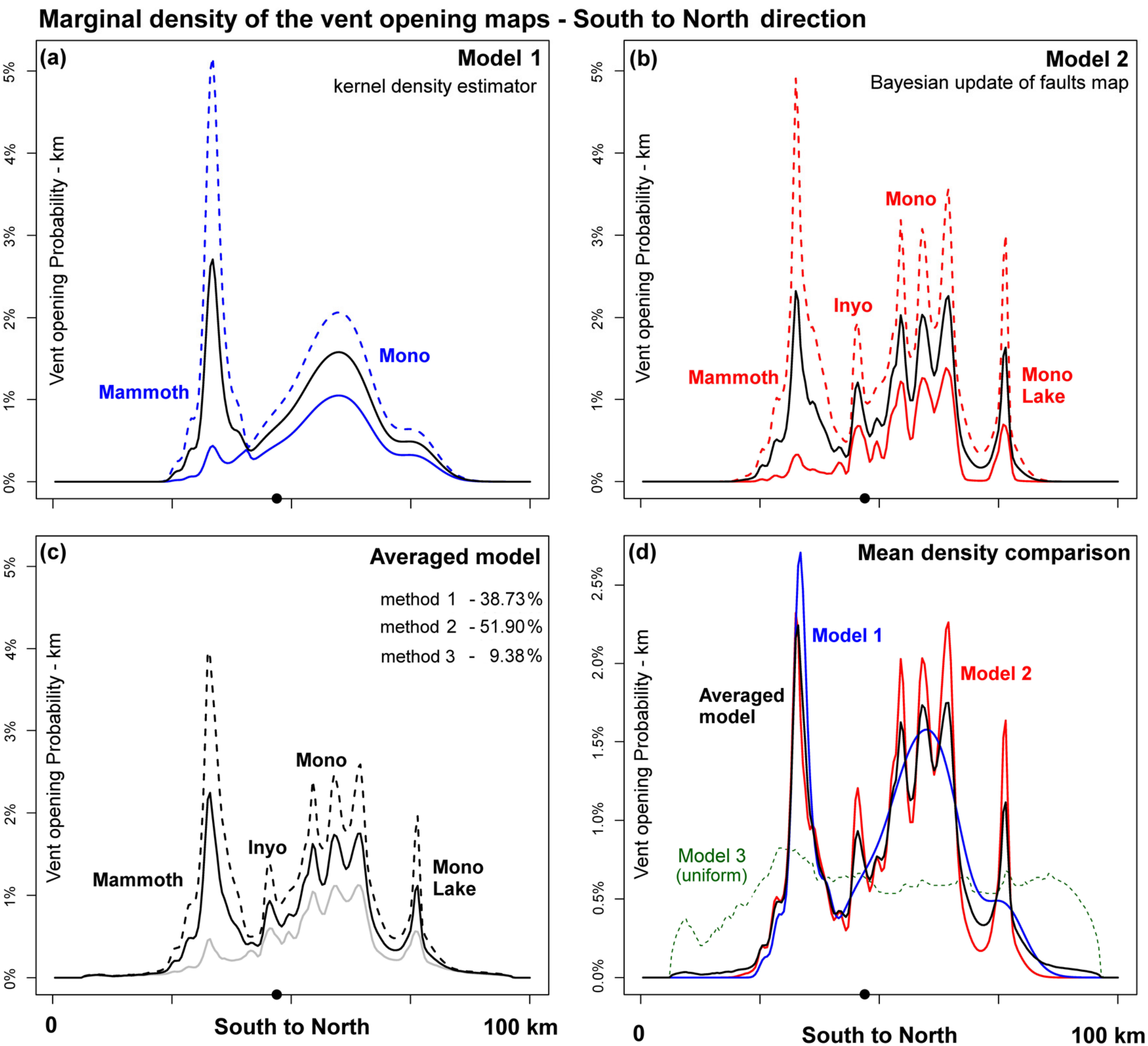

The figure shows the vent opening probability density function along the **South-to-North** direction.

This is a one-dimensional **summary** of the vent opening maps.

Concluding remarks

We have developed a new spatial map of long-term **probability of vent opening**, conditioned on the occurrence of a volcanic eruption in the LVVR region.

Three different statistical models have been combined through a procedure based on a **comparative validation** via the hind-casting of the most recent vent locations.

We have calculated the vent opening probability on the north and south parts of the region, obtaining ~64% and ~36% **probability** respectively, with an **uncertainty** of about ±20%.

The hazard associated with **Mammoth Mountain** should be more fully evaluated, as previously it has tended to be estimated near zero, owing to the age of the edifice as a whole.

Our vent opening forecasts will hopefully help constrain a 'next generation' of volcanic **hazard zonation**, from which will stem improved understanding of **societal vulnerability** to volcano hazards, more targeted **hazard mitigation** strategies, and wise community growth and **development planning**.